

Supplementary Materials for

Light-induced control of protein destruction by opto-PROTAC

Jing Liu, He Chen, Leina Ma, Zhixiang He, Dong Wang, Yi Liu, Qian Lin, Tinghu Zhang,
Nathanael Gray, H. Ümit Kaniskan, Jian Jin*, Wenyi Wei*

*Corresponding author. Email: wwei2@bidmc.harvard.edu (W.W.); jian.jin@mssm.edu (J.J.)

Published 21 February 2020, *Sci. Adv.* **6**, eaay5154 (2020)
DOI: 10.1126/sciadv.aay5154

This PDF file includes:

- Fig. S1. The schematic illustration of the synthesis of opto-pomalidomide and the working model for opto-pomalidomide to achieve light-induced degradation of IKZF1/3.
- Fig. S2. UPLC-MS characterization and the time-dependent uncaging of pomalidomide and opto-pomalidomide.
- Fig. S3. Uncaging of opto-pomalidomide by UVA irradiation leads to active degradation of IKZFs in multiple myeloma cancer cell lines.
- Fig. S4. The schematic illustration of the synthesis of opto-dBET1 and the working model for opto-dBET1 to achieve light-induced degradation of BRDs.
- Fig. S5. UPLC-MS characterization and the time-dependent uncaging of opto-dBET1 by UVA irradiation in vitro.
- Fig. S6. dBET1 inhibits cell proliferation in a CRBN-dependent manner.
- Fig. S7. The schematic illustration of the synthesis of opto-dALK and the working model for opto-dALK to achieve light-induced degradation of ALK fusion proteins.
- Fig. S8. UPLC-MS characterization and the time-dependent uncaging process of opto-dALK.
- Fig. S9. Dose-dependent degradation of ALK fusion proteins by dALK.

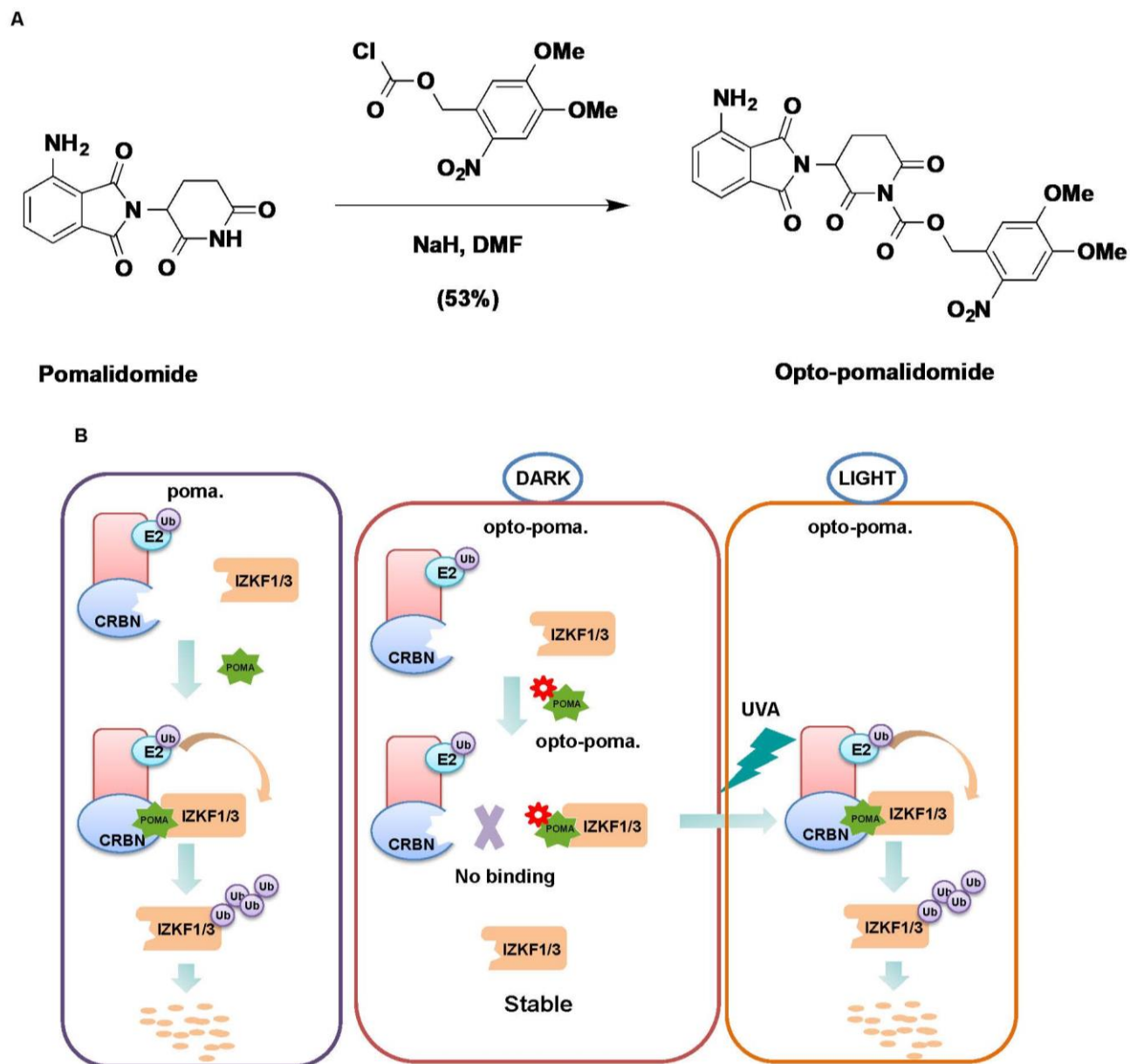


Fig. S1. The schematic illustration of the synthesis of opto-pomalidomide and the working model for opto-pomalidomide to achieve light-induced degradation of IKZF1/3. A) Synthesis of opto-pomalidomide from pomalidomide. B) A schematic illustration for the working model of constitutively active degradation of IKZFs by pomalidomide vs. light inducible degradation of IKZFs by opto-pomalidomide.

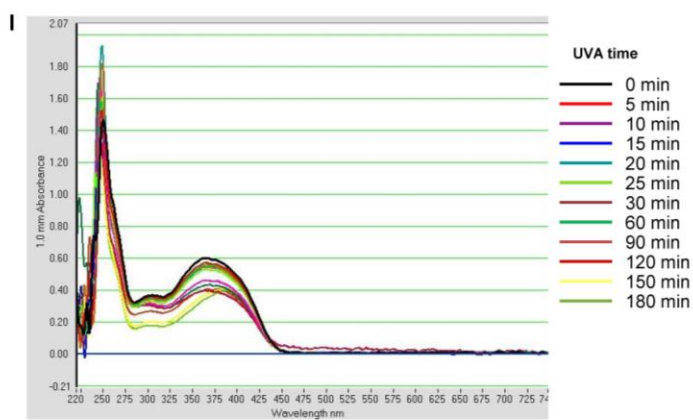
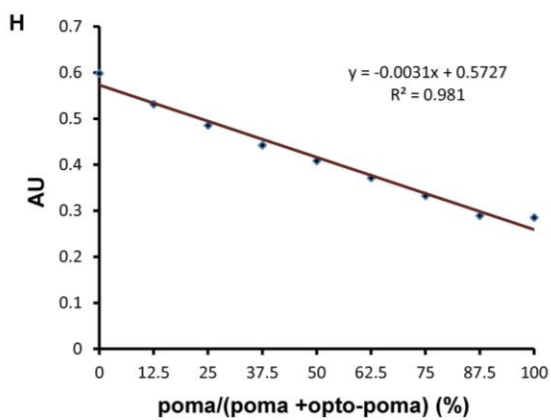
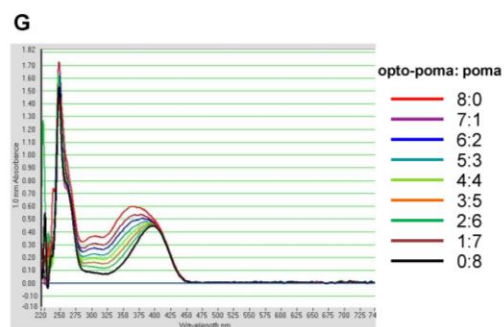
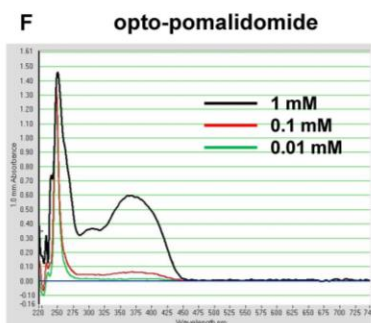
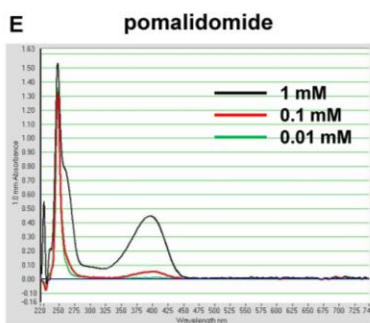
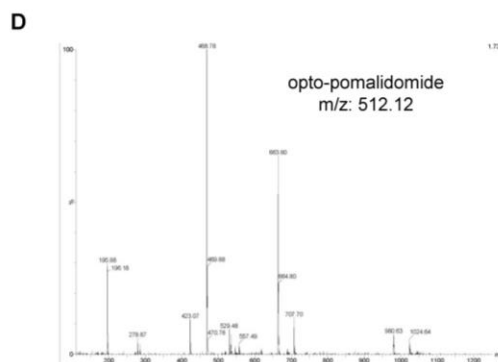
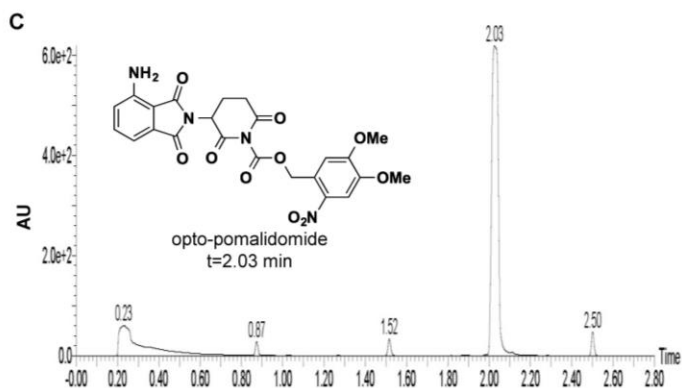
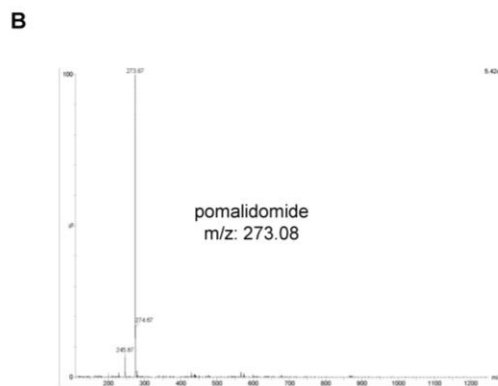
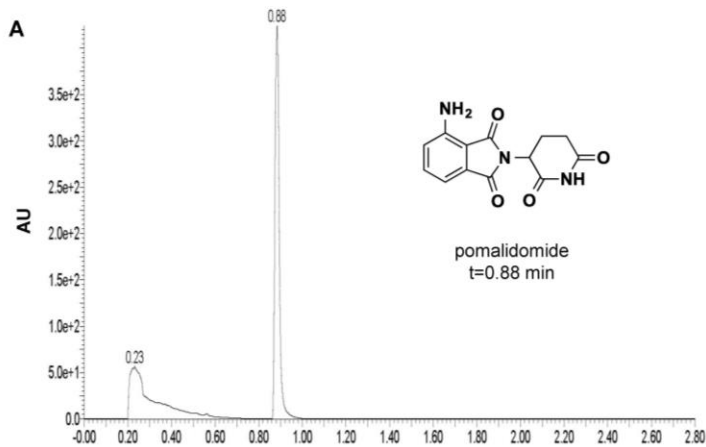


Fig. S2. UPLC-MS characterization and the time-dependent uncaging of pomalidomide and opto-pomalidomide. A) UPLC analysis of pomalidomide. B) Mass spectrum of pomalidomide by UPLC-MS. C) UPLC analysis of opto-pomalidomide. D) Mass spectrum of opto-pomalidomide by UPLC-MS. E) UV-VIS absorption of pomalidomide. F) UV-VIS absorption of opto-pomalidomide. G) UV-VIS absorption of pomalidomide and opto-pomalidomide mixture. H) Standard curve of pomalidomide and opto-pomalidomide mixed at corresponding ratio. I) UV-VIS absorption of opto-pomalidomide after irradiation with UVA (365nm) for indicated time.

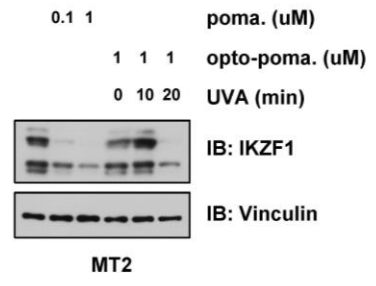
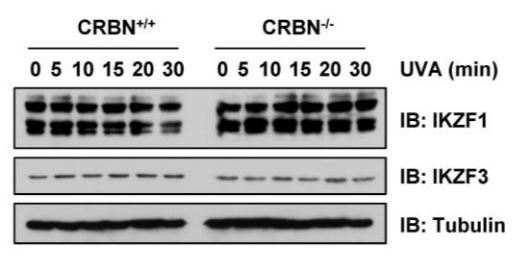
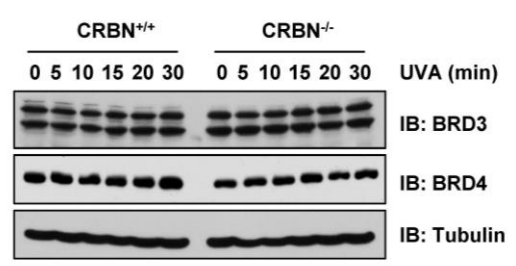
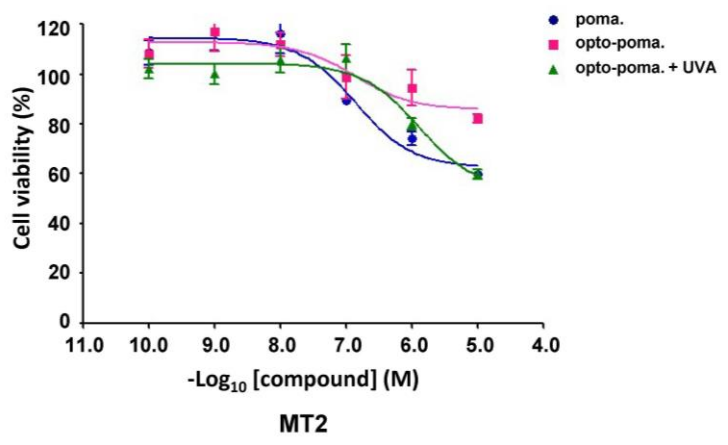
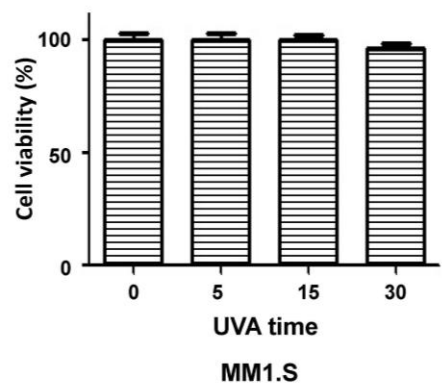
A**B****C****D****E**

Fig. S3. Uncaging of opto-pomalidomide by UVA irradiation leads to active degradation of IKZFs in multiple myeloma cancer cell lines. A) UVA irradiation activates opto-pomalidomide to mediate IKZF1 degradation in MT2 cells. B) UVA irradiation (365nm) alone does not lead to degradation of IKZF1/3 in MM1.S. C) UVA irradiation (365nm) alone does not lead to degradation of IKZF1/3 in 293FT cells. D) UVA irradiation-activated opto-pomalidomide inhibits MT2 cell proliferation in a dose-dependent manner. MT2 cells were treated by pomalidomide vs. opto-pomalidomide with or without UVA irradiation (365 nm) for 15 min, and then subjected to CCK-8 cell viability assay. E) UVA irradiation (365 nm) for 5-30 min has minimal effect on the cell viability of MM1.S cells in the absence of opto-pomalidomide. MM1.S cells were illuminated with UVA for indicated time, and then subjected to CCK-8 cell viability assay.

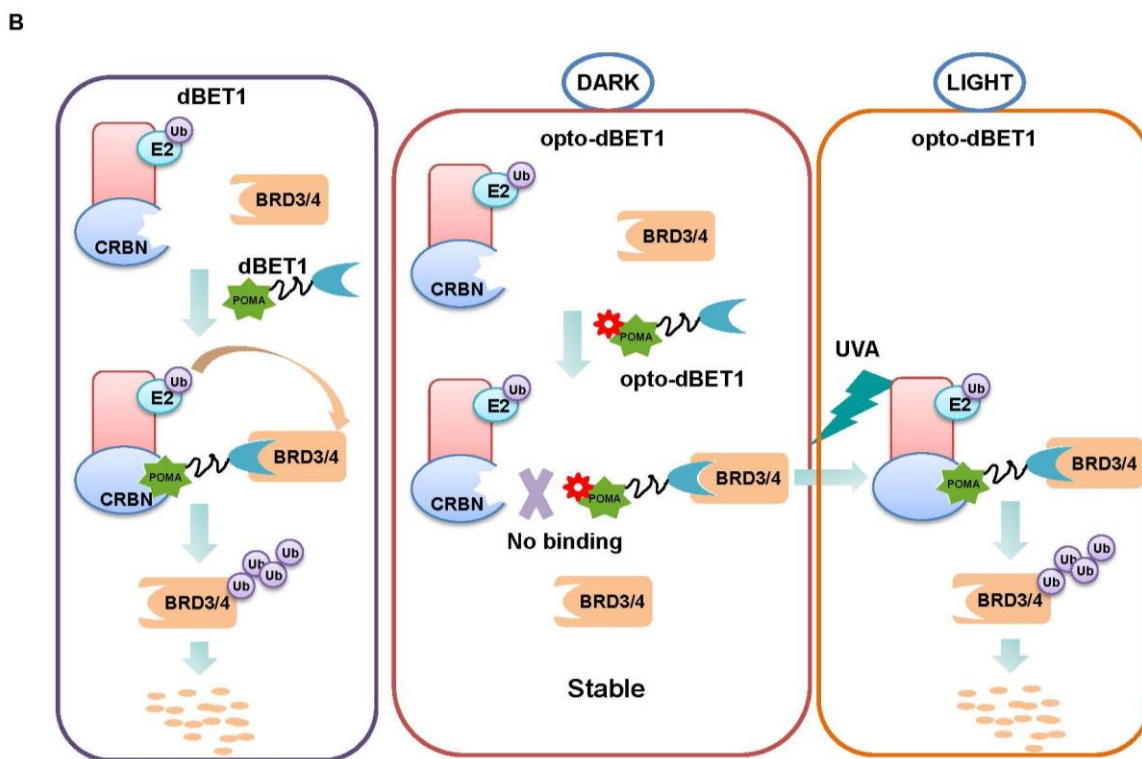
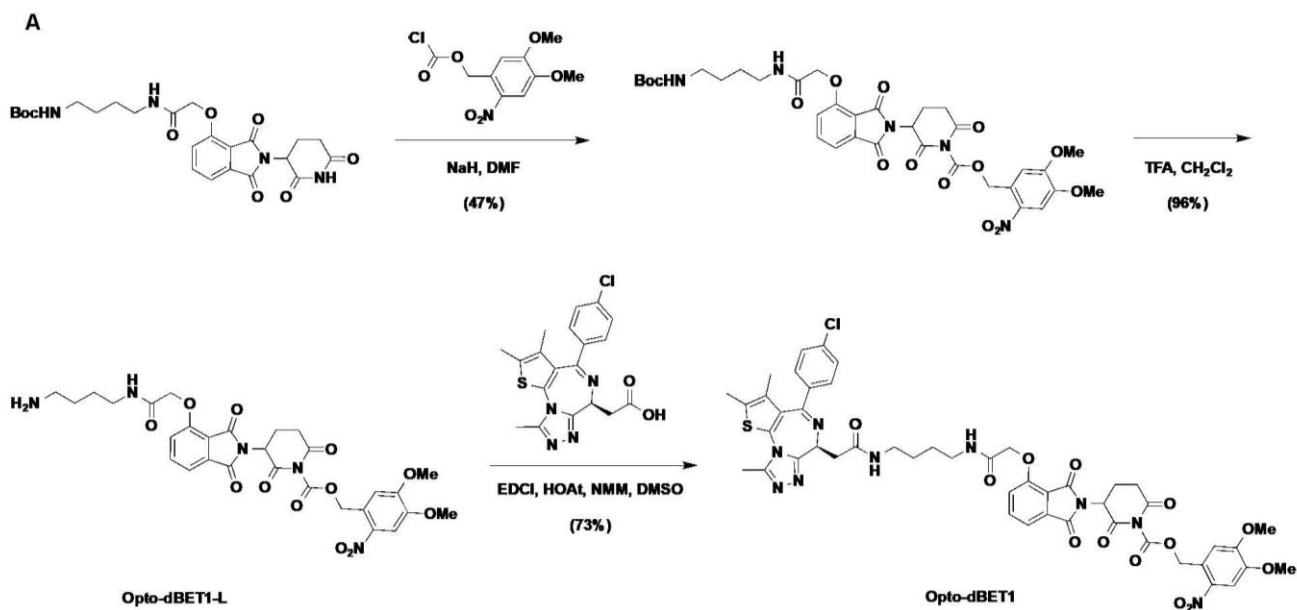


Fig. S4. The schematic illustration of the synthesis of opto-dBET1 and the working model for opto-dBET1 to achieve light-induced degradation of BRDs. A) Synthesis of opto-dBET1. B) A schematic illustration for the working model of dBET1 vs. opto-dBET1 vs. opto-dBET1 + UVA irradiation on promoting degradation of BRDs.

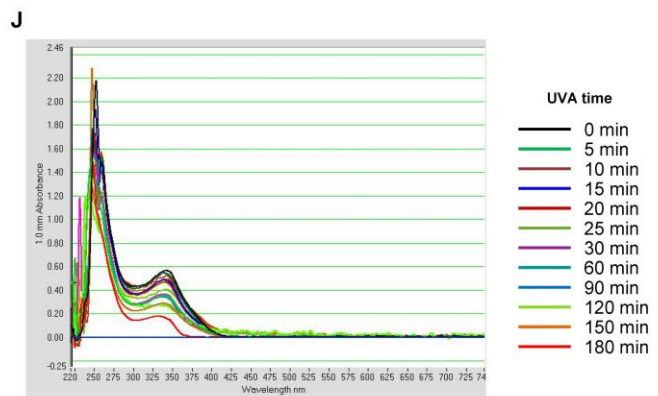
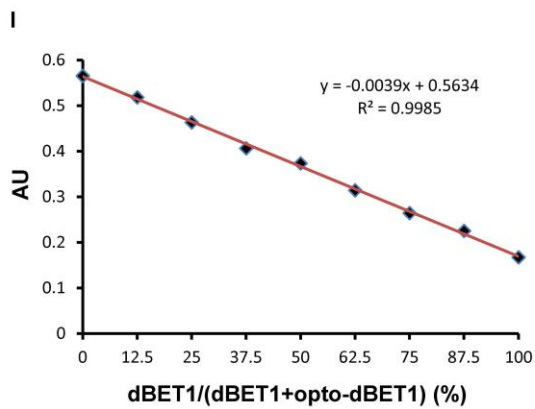
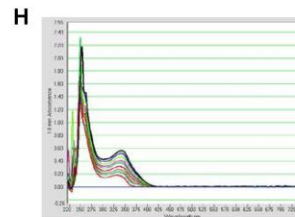
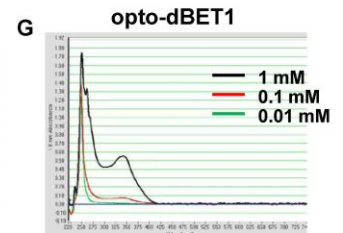
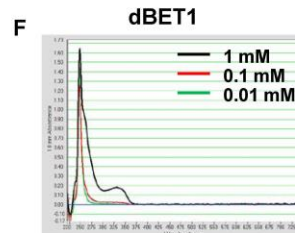
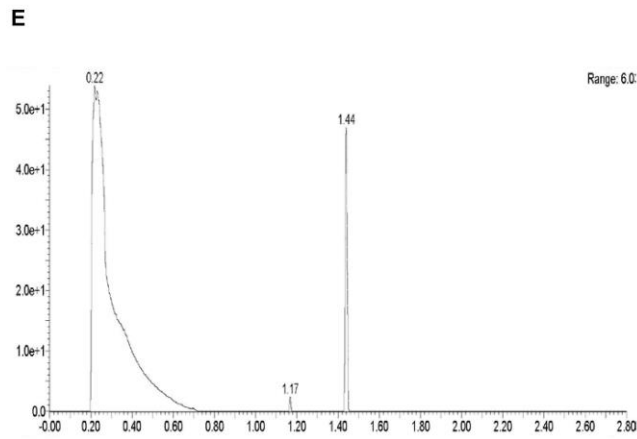
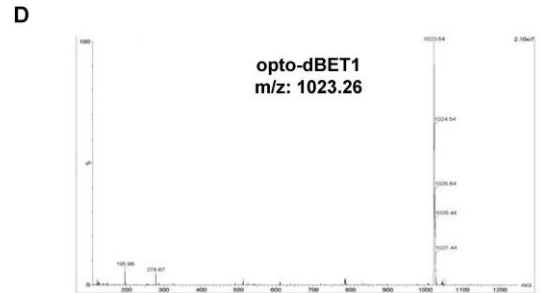
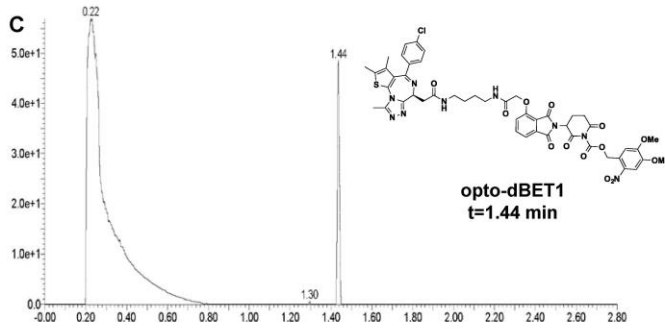
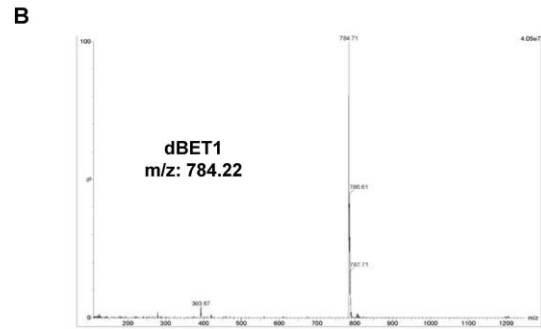
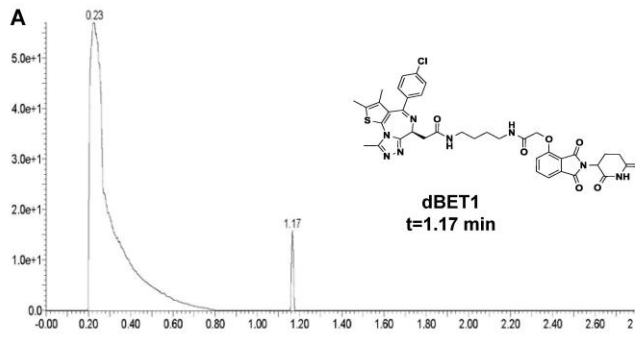


Fig. S5. UPLC-MS characterization and the time-dependent uncaging of opto-dBET1 by UVA irradiation in vitro. A) UPLC analysis of dBET1. B) Mass spectrum of dBET1 by UPLC-MS. C) UPLC analysis of opto-dBET1. D) Mass spectrum of opto-dBET1 by UPLC-MS. E) UPLC analysis of opto-dBET1 after irradiation with UVA (365nm) for 30 minutes. F) UV-VIS absorption of dBET1. G) UV-VIS absorption of opto-dBET1. H) UV-VIS absorption of dBET1 and opto-dBET1 mixture at the corresponding ratio. D. Standard curve of dBET1 and opto-dBET1 at the corresponding ratio. I) UV-VIS absorption of opto-dBET1 after irradiation with UVA (365nm) for indicated time.

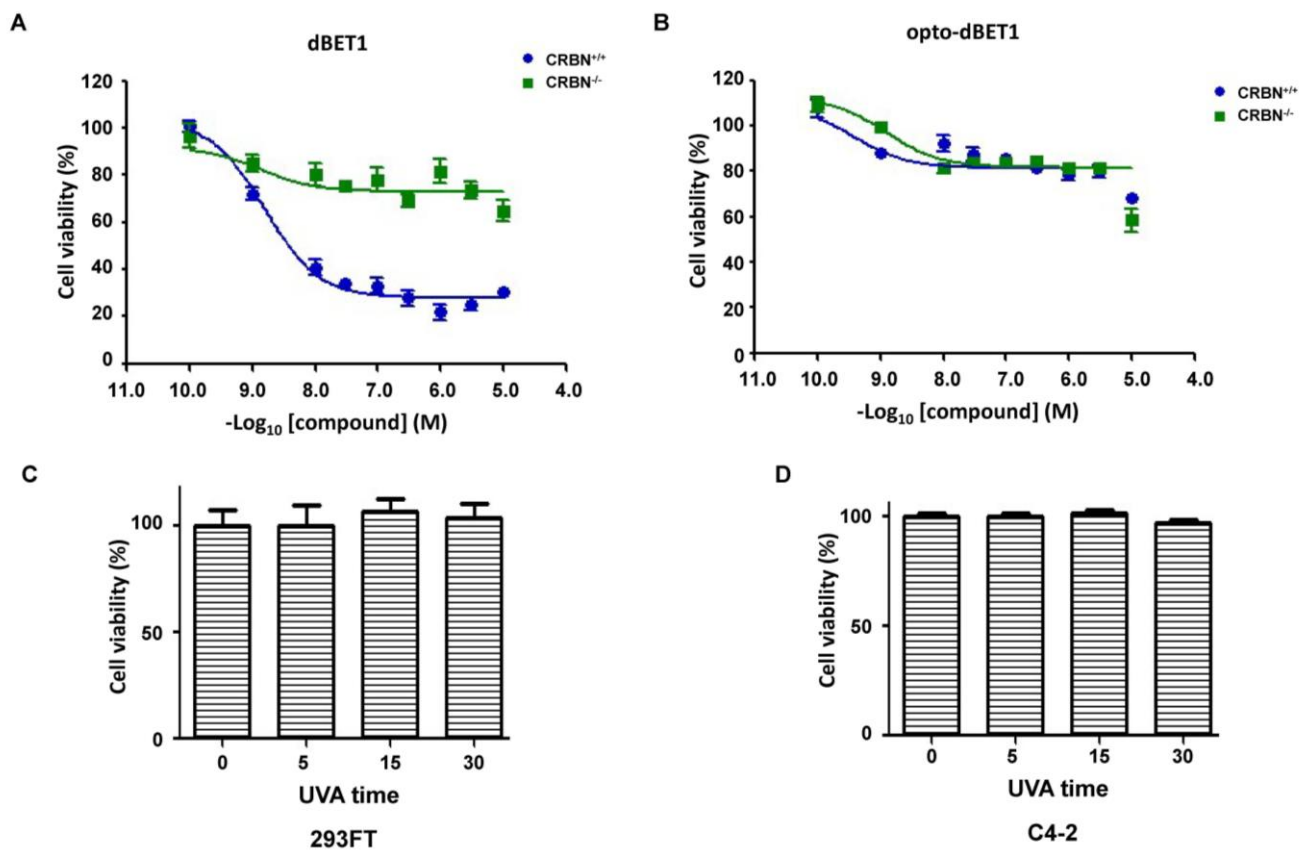


Fig. S6. dBET1 inhibits cell proliferation in a CRBN-dependent manner. A) dBET1 inhibits cell proliferation in 293FT-*CRBN*^{+/+} but not 293FT-*CRBN*^{-/-} cells. B) opto-dBET1 did not inhibit cell proliferation in 293FT-*CRBN*^{+/+} and 293FT-*CRBN*^{-/-} cells. 293FT-*CRBN*^{+/+} and 293FT-*CRBN*^{-/-} cells were treated by dBET1 vs. opto-dBET1 for 72 hours, and then subjected to CCK-8 cell viability assay. C-D) UVA irradiation (365 nm) for 5-30 min has minimal effect on the cell viability of 293FT (C) and C4-2 (D) cells in the absence of opto-dBET1. 293FT and C4-2 cells were illuminated with UVA for indicated time, and then subjected to CCK-8 cell viability assay.

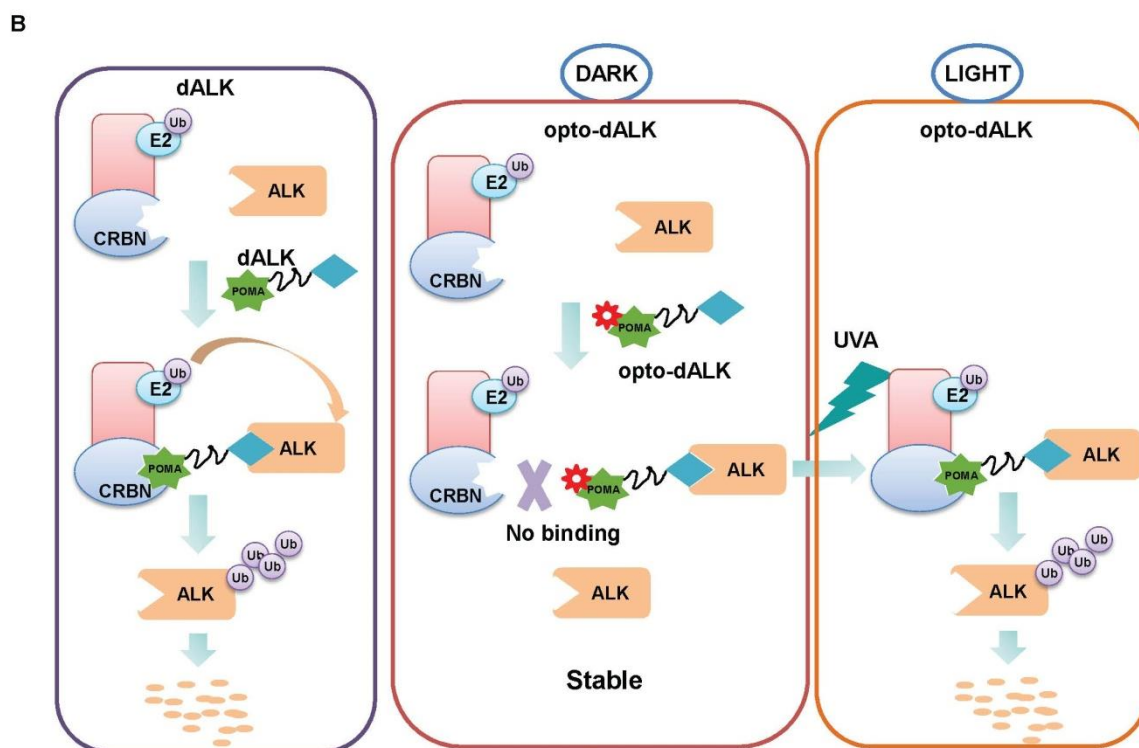
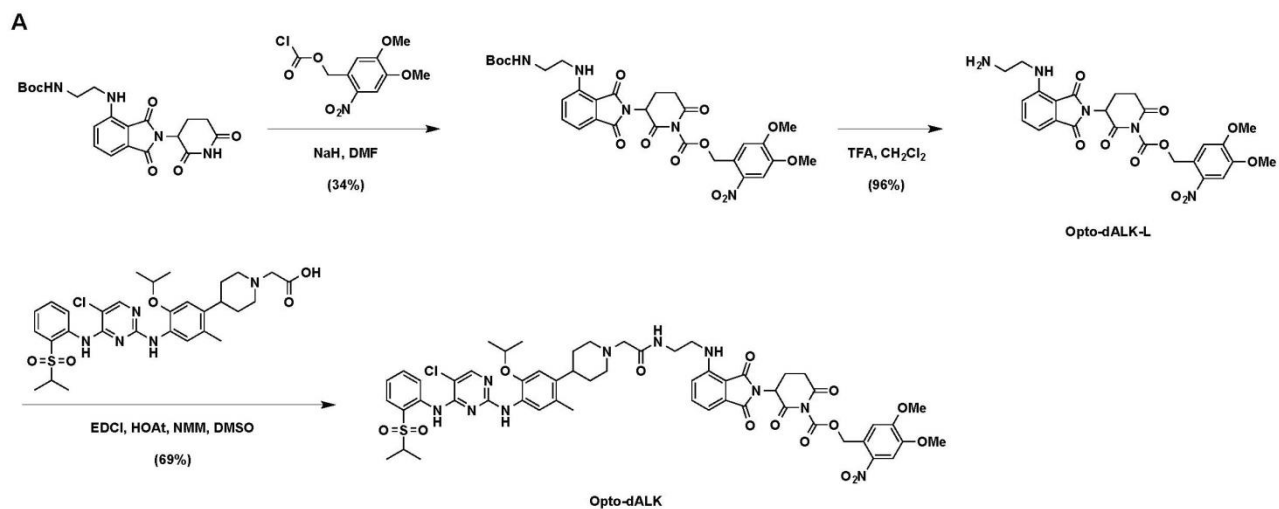


Fig. S7. The schematic illustration of the synthesis of opto-dALK and the working model for opto-dALK to achieve light-induced degradation of ALK fusion proteins. A) Synthesis of opto-dALK. B) A schematic illustration for the working model of dALK vs. opto-dALK vs. opto-dALK + UVA irradiation (365nm) on promoting the degradation of ALK fusion proteins.

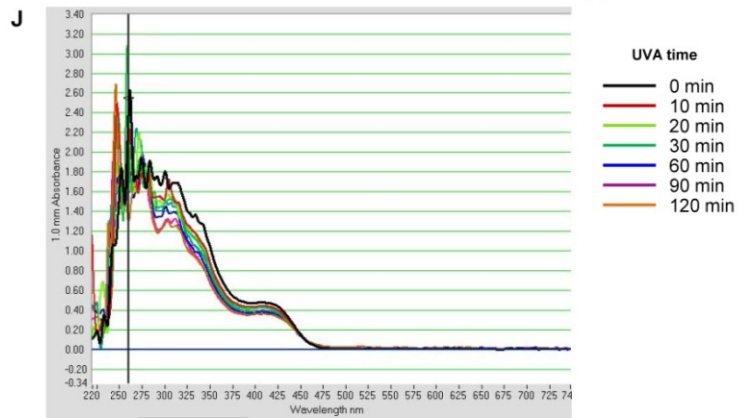
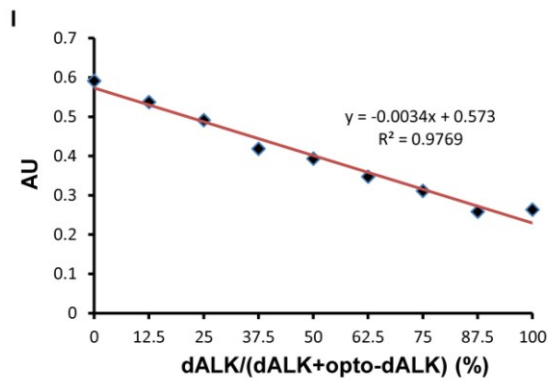
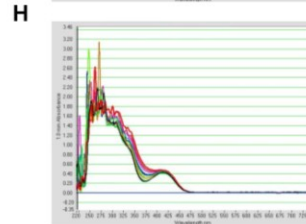
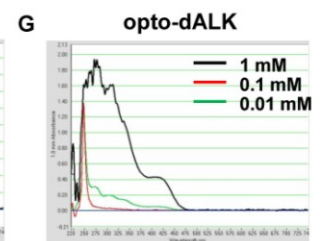
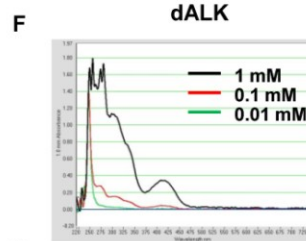
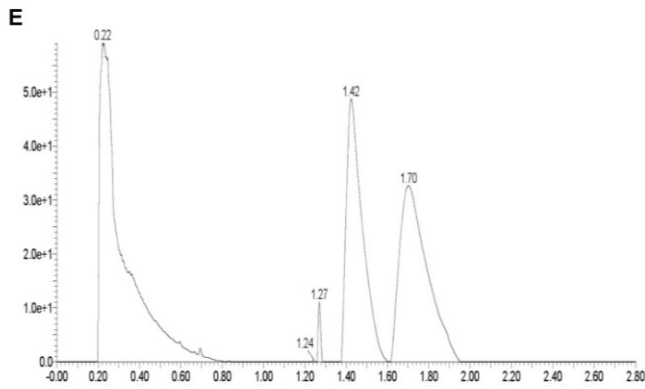
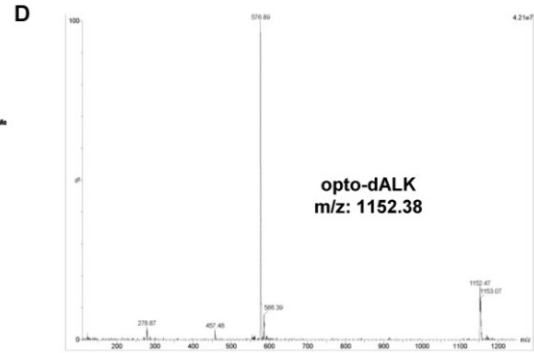
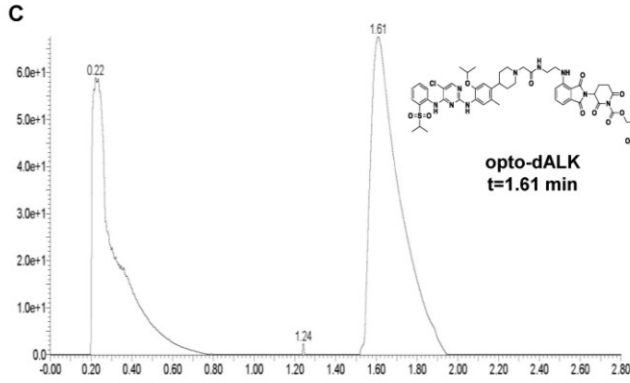
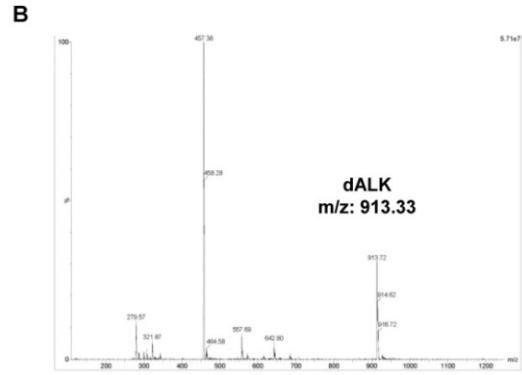
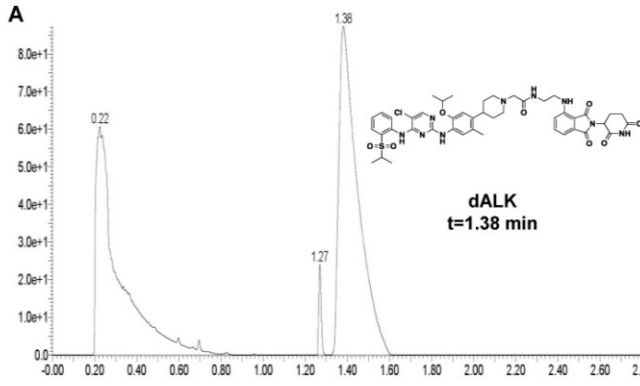


Fig. S8. UPLC-MS characterization and the time-dependent uncaging process of opto-dALK. A) UPLC analysis of dALK. B) Mass spectrum of dALK by UPLC-MS. C) UPLC analysis of opto-dALK. D) Mass spectrum of opto-dALK by UPLC-MS. E). UPLC analysis of opto-dALK after irradiation with UVA (365nm) for 30 minutes. F) UV-VIS absorption of dALK. G) UV-VIS absorption of opto-dALK. H) UV-VIS absorption of dALK and opto-dALK mixture at corresponding ratio. I) Standard curve of dALK and opto-dALK mixed at corresponding ratio. J) UV-VIS absorption of opto-dALK after irradiation with UVA (365nm) for indicated time.

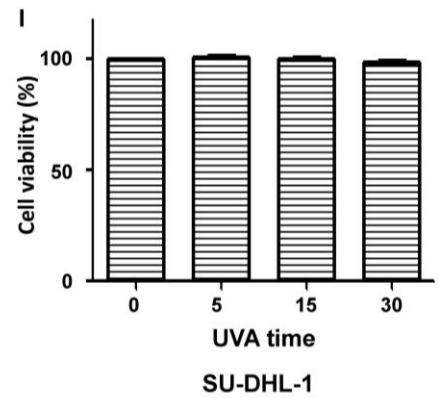
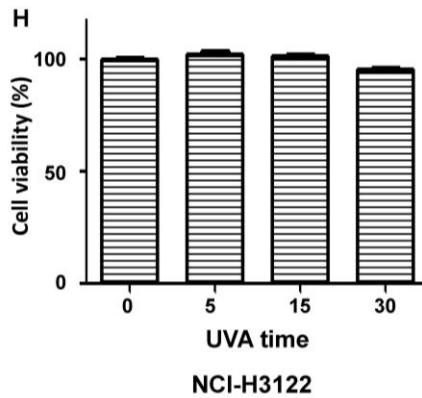
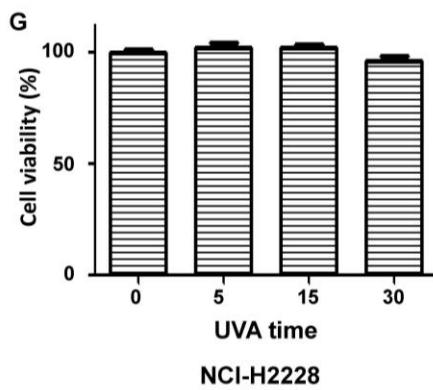
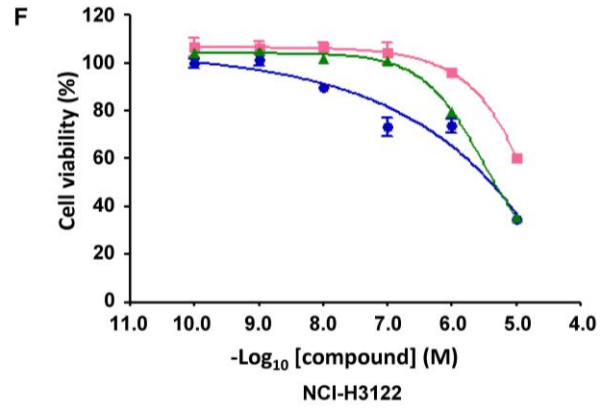
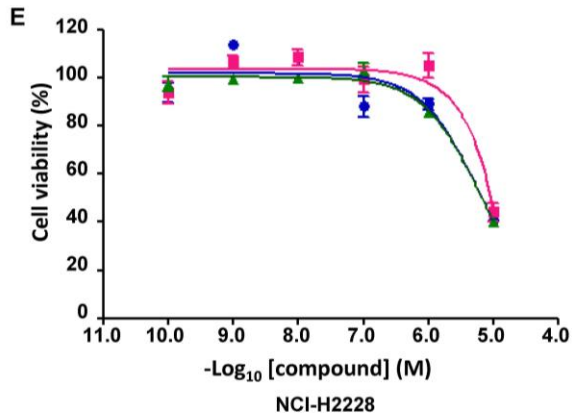
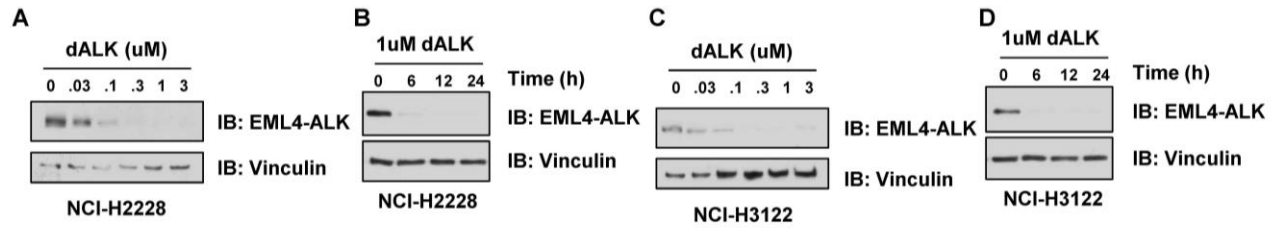


Fig. S9. Dose-dependent degradation of ALK fusion proteins by dALK. A-D) dALK promotes the degradation of EML4-ALK fusion proteins in NCI-H2228 (A, B) and NCI-H3122 (C, D) NSCLC cell lines. NCI-H2228 and NCI-H3122 were treated with dALK at indicated dose or for indicated time, and then subjected to analysis of the level of EML-ALK fusion protein. E-F) The cell proliferation of NCI-H2228 (E) and NCI-H3122 (F) NSCLC cell lines was relative resistant to ALK degrader. NCI-H2228 and NCI-H3122 NSCLC cell lines were treated by dALK vs. opto-dALK with or without UVA irradiation, and then subjected to CCK-8 cell viability assay. G-I) UVA irradiation alone (365 nm) for 5-30 min has minimal effect on the cell viability of NCI-H2228 (G), NCI-H3122 (H) and SU-DHL-1 (I) cells in the absence of opto-ALK. NCI-H2228, NCI-H3122 and SU-DHL-1 cells were illuminated with UVA for indicated time, and then subjected to CCK-8 cell viability assay.